Table 1. Ethylene Hydration: Comparison of Backmix and Tubular Reactors

	Backmix reactor	Tubular reactor
Mole ratio C_2H_4: H_2O	2:1	2:1
Reaction pressure, N/m^2	7 E + 06	7 E + 06
Reaction temperature, °K	543	543
Impeller speed, rev/min	220	—
Catalyst bed c-s, A, m^2	0.0020	0.00027
Catalyst bed depth, L, m	0.0445	2.1336
Space velocity, SV vol/vol/s	0.555	0.5555
Mass velocity, $G = W/A$ kg/m$^2 \cdot$ s	3.63	1.34†
Mass flow rate, W kg/s	0.0074*	0.00036
$NR_e = DpG/\mu$	2 257	833

* From Figure 2, using $\rho = 39.237$ kg/cm^3.
† For a tubular reactor, $G/SV = M_{av}\, L/22.4$.

is controlled by impeller speed and the latter by the feed rate. Assuming the flowing gases to be incompressible for small pressure drops in a backmix reactor, Berty et al. (1969) varied gas density, impeller speed, and L/D_p ratios and measured pressure drop as a function of flow rate. It follows, then, that if any two of the following three parameters, are defined, the third can be estimated by the use of Figure 2 (L/D_p ratio, impeller speed, flow rate).

By extrapolating the data of Berty et al. in Figure 2, a determination of flow rate, and finally mass velocity, are tabulated in Table 1. Comparing the operating conditions in the backmix versus tubular reactor, it can be seen that while space velocities are identical in both reactors, mass velocity is approximately three times higher in the backmix reactor. What is more striking is the high mass flow rate inside the backmix reactor, some twenty times that in the tubular reactor. This greater agitation is responsible for the rapid loss of phosphoric acid and the concomitant loss in catalytic activity and explains the shorter duration of a catalytic life test in the backmix reactor, about one sixteenth the time required in a tubular reactor.

ACKNOWLEDGMENT

The authors wish to thank Union Carbide Corporation for permission to publish this work.

NOTATION

A = cross-sectional area of the catalyst bed, m^2
D_p = equivalent diameter of catalyst particles, m
F = flow rate, kg mole/s
G = mass velocity, kg/m$^2\cdot$s
k_1 = reaction rate constant for ethylene consumption, N$\cdot$kg/m$\cdot$s at 550°K
k_2 = reaction rate constant for diethyl ether formation, N$\cdot$kg/m$\cdot$s at 550°K
L = catalyst bed depth, m
M_{av} = average molecular weight of vapor
N_{Re} = Reynolds number = D_pG/μ
P = pressure, total, N/m^2
$P_{C_2H_4}$ = partial pressure of ethylene, N/m^2
P_{H_2O} = partial pressure of water, N/m^2
P_{Et_2O} = partial pressure of ethanol, N/m^2
P_{EtOH} = partial pressure of ethanol, N/m^2
R = universal gas constant = $8{\cdot}3 \times 10^{-3}$ J/kg mole
r_1 = rate of ethylene consumption, kg mole/m$^3\cdot$s of catalyst bed
r_2 = rate of diethyl ether formation, kg mole/m$^3\cdot$s of catalyst bed
SV = space velocity = F/V, std m^3/s/m^3 of catalyst bed
T = reaction temperature, °K
T^* = temperature function = $1/R[1/T - 1/550]$, kg mole/J
V = volume of reactor, m^3
x_1 = mole fraction of ethylene
x_2 = mole fraction of diethyl ether
W = mass flow rate, kg/s
ρ = vapor density, kg/m^3
μ = viscosty, N$\cdot$s/m^2

LITERATURE CITED

Berty, J. M., et al., "Reactor for Vapor Phase Catalytic Studies," paper presented at the Sixty-Fourth National Meeting of the AIChE, New Orleans, La. (Mar. 16, 1969).

Foster, R. D., and J. R. Nelson, Union Carbide Corporation, unpublished results (1975).

Millidge, A. F., in *Ethylene and its Industrial Derivatives,* S. A. Miller, ed., p. 717, Ernest Benn, Ltd., London, England (1969).

Whitmore, F. C., "Mechanism of the Polymerization of Olefins by Acid Catalysts," *Ind. Eng. Chem.*, 26, 94 (1934).

Manuscript received December 4, 1978; revision received March 2, and accepted March 23, 1979.

An Approximate Solution for the Graetz and Lévêque Problems from the Advancing Front Theory

PIETER STROEVE and R. SRINIVASAN

Department of Chemical Engineering
State University of New York at Buffalo
Amherst, New York 14260

The freezing of a lake, the regeneration of coked reformer catalyst, the tarnishing of a metal surface, the impregnation of supports with catalytically active materials, or the oxygenation of venous blood are examples of moving boundary problems. These problems involve the transport of heat or mass to a moving boundary. The

---

Pieter Stroeve is also with the Department of Biophysical Sciences, State University of New York at Buffalo, Buffalo, New York 14214.

0001-1541-80-2719-0135-$00.75. © The American Institute of Chemical Engineers, 1980.

location of the moving boundary depends on the rate of transport of the diffusing quantity brought to it. Often, moving boundary problems are described by nonlinear differential equations which only have exact analytical solutions in special cases, and, consequently, these problems are solved by numerical methods. However, when the rate of disappearance of the diffusing quantity is fast, the solution reduces to finding the thickness of the boundary layer by using an integral method. The advancing front theory is an approximate technique which has been used extensively in physiological situations such as the oxygenation of fatigued muscle (Hill, 1928) or the design of artificial oxygenators (Lightfoot, 1968). Comparisons of predictions from the advancing front theory with numerical techniques have shown that the advancing front theory gives accurate results for a wide variety of parameters (Spaan, 1973).

In this communication, we show by plotting the advancing front theory in dimensionless form that the theory can be extended to the nonreactive situation and that the theory gives a reasonable approximation for the classical Graetz and Lévêque problems. The approximate solution is a simple analytical solution. The application of the advancing front theory to the nonreactive situation and the comparison to the results obtained from both the Lévêque and Graetz problems gives quantitative values of the accuracy of the advancing front theory for the worst possible case.

THEORY

We shall consider a reactive fluid (containing reactant B) flowing between two flat parallel membranes in fully developed laminar flow along the z direction. The membranes are semipermeable and allow another reactant (reactant A) at concentration C_o to diffuse through the membrane and into the fluid. Inside the fluid, reactant A reacts instantaneously with the reactant B present in the fluid. The situation is analogous to the problem of oxygen transport to blood flowing in a parallel plate membrane oxygenator. In the oxygenator, the oxygen converts hemoglobin to oxyhemoglobin. We will consider this specific problem, but one should keep in mind that the equations derived are general for any reactive situation of the form A + B → AB. For the artificial oxygenator, one needs to determine the oxygen mass transfer rate into the blood and the mixing cup concentration of oxyhemoglobin as a function of channel length z.

We consider the case where the membranes are located at $x = 0$ and $x = 2d$ on a xz-axis. Assuming steady state conditions, the oxygen balance is given as (Buckles et al., 1968; Dorson, 1970; Spaan, 1973)

$$v_z \frac{\partial}{\partial z}(4c_T S + C) = D_c \frac{\partial^2 C}{\partial x^2} + 4c_T D_{Hb} \frac{\partial^2 S}{\partial x^2} \quad (1)$$

Here $4c_T S$ is the concentration of reacted hemoglobin in the form of tetramer. The boundary conditions are

$$x = d, \frac{\partial C}{\partial x} = 0, \quad \text{all } z \quad (2)$$

$$x = 0, \quad C = C_o, \quad z \geq 0 \quad (3)$$

$$z < 0, \quad S = S_i, \quad C = C_i, \quad \text{all } x \quad (4)$$

It is assumed that the membranes are highly permeable and have negligible resistance to mass transfer. Equation (1) can be made dimensionless so that

$$v_z^* \frac{\partial}{\partial z^*}(C^* + c_T^* S) = \frac{\partial^2 C^*}{\partial y^2} + D^* \frac{\partial^2 S}{\partial y^2} \quad (5)$$

A solution which takes into account the nonlinear saturation curve would have to be numerical. However, the advancing front theory can be used to obtain approximate solutions, particularly when the concentration C_o is large to cause full saturation of hemoglobin ($S = 1$). The major assumptions in the theory can be summarized as follows:

1. Axial diffusion is negligible in comparison to axial convection.
2. The reaction of oxygen with hemoglobin is instantaneous.
3. The oxygen concentration profile in the saturated layer (that is, the oxyhemoglobin layer) is linear.

The assumptions lead to

$$y \leq p, \quad S = 1, \quad \text{and} \quad C^* = 1 - \left(\frac{1 - C_i^*}{p}\right) y \quad (6)$$

and

$$y > p, \quad S = S_i, \quad \text{and} \quad C^* = C_i^* \quad (7)$$

where p is the dimensionless thickness of the saturated layer $p = \xi/d$. The velocity profile is given by

$$v_z^* = \frac{3}{2}(2y - y^2) \quad (8)$$

Division of Equation (5) into saturated and unsaturated regions, the introduction of Equations (6) through (8), and subsequent integration leads to

$$z^* = 3\left[p^3\left(\frac{1}{9} + \frac{Q}{6}\right) - p^4\left(\frac{1}{32} + \frac{Q}{16}\right)\right] \quad (9)$$

and

$$\overline{S} = S_i + (1 - S_i)\left(\frac{3}{2}p^2 - \frac{1}{2}p^3\right) \quad (10)$$

The parameter Q is given by

$$Q = \frac{4c_T(1 - S_i)}{\frac{1}{2}(C_o - C_i)} \quad (11)$$

and is an indication of the strength of the reaction; that is, it is the ratio of total hemoglobin available for reaction divided by ½ of the maximum oxygen concentration difference. For a given average mixing cup saturation $\overline{S}$, Equations (9) and (10) allow calculation of both the length z^* necessary to attain the saturation and the thickness of the saturated front p measured from the membranes into the blood at position z^*.

RESULTS AND DISCUSSION

The theoretical results of the advancing front theory can be expressed in various ways. For example, Lightfoot (1968) plotted $(\overline{S} - S_i)/(1 - S_i)$ vs. $(2/Q)z^*$, while Spaan (1973) plotted $\overline{S}$ vs. z^*. However, since we are dealing with mass transfer in a conduit, the oxygenation process can be characterized also in terms of a plot of the Sherwood number vs. the dimensionless axial distance. The mixing cup concentration is given by

$$C_B = \int_0^1 C v^* dy = \frac{3}{2}\left\{\int_0^p \left[C_o - (C_o - C_i)\frac{y}{p}\right] [2y - y^2]dy + \int_p^1 C_i[2y - y^2]dy\right\} \quad (12)$$

which becomes

$$C_B = C_i + (C_o - C_i)\left(\frac{p^2}{2} - \frac{p^3}{8}\right) \qquad (13)$$

The mass transfer rate per unit area is given by

$$-D_c \frac{dC}{dx}\bigg|_{x=0} = D_c \frac{(C_o - C_i)}{pd} \qquad (14)$$

The local fluid side mass transfer coefficient is defined as

$$k_z(C_o - C_B) = -D_c \frac{dC}{dx}\bigg|_{x=0} \qquad (15)$$

From the above equations, the local fluid side Sherwood number is

$$Sh_z = \frac{k_z 2d}{D_c} = \frac{2}{\left(p - \frac{p^3}{2} + \frac{p^4}{8}\right)} \qquad (16)$$

With Equations (9) and (16), plots of Sh_z vs. z^* can be obtained for different values of Q as shown in Figure 1. The figure shows that with increasing values of Q, the local fluid side Sherwood number increases. This phenomenon is consistent with the concept of the enhancement of the mass transfer rate due to the chemical reaction (Danckwerts, 1970) and, as a consequence, makes the figure useful to ascertain the effect of chemical reaction on the mass transfer rate. At large values of z^*, the curves decrease to a constant value of 3.200. This is the point that p becomes equal to 1 and $\overline{S} = 1$, so that reaction ceases. For larger dimensionless lengths z^*, the oxygen concentration is fully developed in triangular form. Included in the figure is a plot of the Sh_z vs. z^* for the nonreactive case obtained by Colton et al. (1971) for the classical Lévêque and Graetz problems. For this case, the curve asymptotes to a value of 3.770, where the concentration C assumes a fully developed curvilinear form. The nonreactive case for the advancing front theory occurs for the extreme value of $Q = 0$. The close match of the advancing front theory with the Graetz and Lévêque problems is surprising; the maximum deviation is 15.1% which occurs for the asymptotic values. In essence, the difference between the exact Graetz problem and the advancing front theory is that the latter linearizes the concentration profile for C, while the former forms a curvilinear profile.

Further investigation of the advancing front theory at small values of z^* (where p approaches zero) yields a solution for the local fluid side Sherwood number ($Q = 0$):

$$Sh_z = 1.387\, z^{*-1/3} \qquad (17)$$

The relationship obtained from the Lévêque analysis is given by Colton et al. (1971) as

$$Sh_z = 1.553\, z^{*-1/3} \qquad (18)$$

Comparison of Equations (17) and (18) shows that the advancing front theory yields an approximate solution for the Lévêque problem which differs by only 10.7%. Application of the advancing front theory to the nonreactive case $Q = 0$ yields a single analytical solution that is a reasonable approximation to both the Lévêque and Graetz problems. The Graetz problem is computationwise a time consuming problem, since one deals with an infinite series, and consequently the approximate solution is useful because of its simplicity. In addition, the application of the advancing front theory to the extreme case of $Q = 0$ shows that, at worst, the solution has an error of approximately 11 to 15%. For values of Q greater than zero, the results improve as has been shown experimentally by Dorson and Voorhees (1976) as long as the basic assumptions are fulfilled.

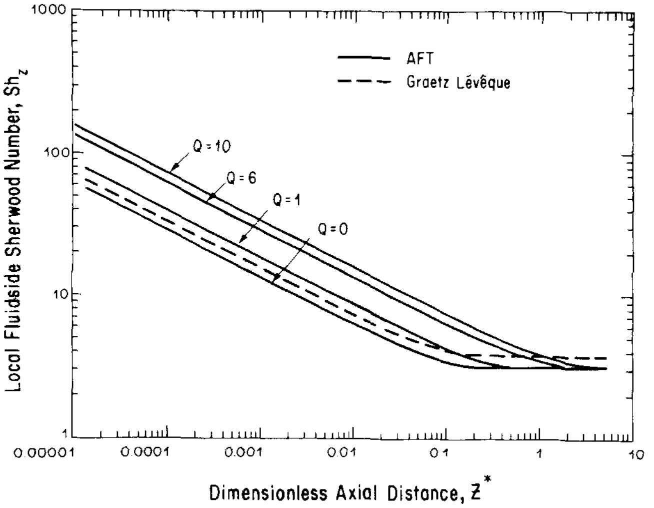

Figure 1. Dimensionless plot of the local fluid side Sherwood number as a function of the Graetz number z^* for the advancing front theory (AFT) and the Graetz and Lévêque solutions.

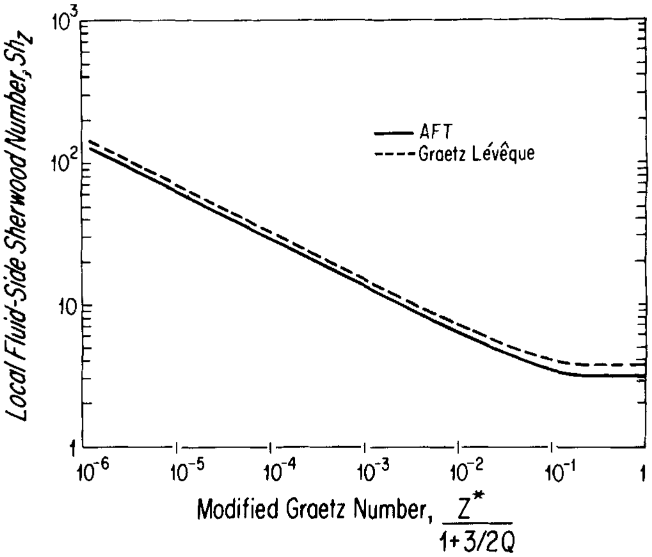

Figure 2. Dimensionless plot of the local fluid side Sherwood number as a function of the modified Graetz number.

A Lévêque type of form can also be obtained from the advancing front theory for reactive cases when z^* is small. From Equations (9) and (16), one obtains

$$Sh_z = 1.387\left(\frac{z^*}{1 + \frac{3}{2}Q}\right)^{-1/3} \qquad (19)$$

Based on this relationship, it is possible to define an enhancement factor E for mass transport due to the chemical reaction

$$E = \frac{Sh_z(Q)}{Sh_z(Q = 0)} = \left(1 + \frac{3}{2}Q\right)^{1/3} \qquad (20)$$

for small z^*. The form of Equation (19) suggests that another appropriate dimensionless number for correlating the results of the advancing front equation is $z^*/(1 + 3Q/2)$. Figure 2 shows a plot of Sh_z vs. this new parameter which can be considered to be a modified Graetz number for reaction. The curves for any value of Q collapse almost completely in one single curve; there is a small difference in the bend. Again, the difference between the advancing front theory and the Graetz and Levêque solutions (which is applicable to $Q = 0$) is small. As a consequence, the Graetz-Lévêque solution on this type of plot can also be used for reactive problems ($Q > 0$) with an expected difference with the advancing front theory of 11 to 15% maximum.

NOTATION

C = concentration of oxygen (A) in the fluid, moles/cm^3
C_i = initial value of C, moles/cm^3
C_o = value of C at $x = 0$ and $x = 2d$, moles/cm^3
C_B = cup mixing concentration of oxygen (A), defined by Equation (13), moles /cm^3
c_T = total concentration of B in all forms in the fluid, moles/cm^3
$2d$ = film thickness, cm
D_c = diffusion coefficient of oxygen (A) in the fluid, cm^2/s
D_{Hb} = diffusion coefficient of hemoglobin (B) in the fluid, cm^2/s
k_z = local mass transfer coefficient, defined by Equation (15), cm/s
v_z = velocity of fluid in the z direction, cm/s
v_{av} = average velocity of blood in the z direction,

$$= \frac{1}{d}\int_0^d v_z \cdot dx, \text{ cm/s}$$

x = distance in the transverse direction, cm
z = distance in the direction of flow, cm
z^* = Graetz number
ξ = thickness of the saturated layer, cm

Dimensionless Quantities

C^* = C/C_o
c_T^* = $4c_T/C_o$
D^* = $D_{Hb} \cdot c_T^*/D_c$
E = enhancement factor, defined by Equation (20)
p = dimensionless thickness of saturated layer, $p = \xi/d$
Q = reaction strength parameter, defined by Equation (11)
S = fractional saturation of total B in AB form
S_i = initial value of S
$\overline{S}$ = mixing cup S
Sh_z = local Sherwood Number, defined by Equation (16)
v^* = v_z/v_{av}
y = x/d
$z^* = \dfrac{zD_c}{v_{av}d^2}$

LITERATURE CITED

Buckles, R. G., E. W. Merrill, and E. R. Gilliland, "An Analysis of Oxygen Absorption in a Tubular Membrane Oxygenator," *AIChE J.*, **14**, 703 (1968).
Colton, C. K., K. A. Smith, P. Stroeve, and E. W. Merrill, "Laminar Flow Mass Transfer in a Flat Duct with Permeable Walls," *ibid.*, **17**, 773 (1971).
Danckwerts, P. V., *Gas-Liquid Reactions*, McGraw-Hill, New York (1970).
Dorson, W. J., "Oxygenation of Blood for Clinical Applications," in *Blood Oxygenation*, E. D. Hershey, ed., Plenum Press, New York (1970).
Dorson, W. J. and M. E. Voorhees, "Analysis of Oxygen and Carbon Dioxide Transfer in Membrane Lungs," in *Membrane Lungs and Acute Respiratory Failure*, W. M. Zapol and J. Quist, ed., p. 43, Hemisphere, Washington, D.C. (1976).
Hill, A. V., "Diffusion of Oxygen and Lactic Acid Through Tissues," *Proc. Royal Soc. London, Ser.*, **B104**, 39 (1928).
Lightfoot, E. N., "Low Order Approximations for Membrane Blood Oxygenators," *AIChE J.*, **14**, 669 (1968).
Spaan, J. A. E., "Transfer of Oxygen into Hemoglobin Solution," *Pflügers. Arch.*, **342**, 289 (1973).

Manuscript received November 9, 1978, and accepted March 20, 1979.

Transient and Steady State Characteristics of a Gaseous Reactant in Catalytic Fluidized-Bed Reactors

LIANG-SHIH FAN and L. T. FAN

Department of Chemical Engineering
Kansas State University
Manhattan, Kansas 66506

Many models have been proposed for describing the performance of a fluidized-bed reactor. These include two-phase models (Kato and Wen, 1969; Fryer and Potter, 1972*a*) and three-phase models (Kunii and Levenspiel, 1968; Fryer and Potter, 1972*b*). More often than not, a simplified flow pattern of plug flow or complete mixing is assumed in representing the fluid flow behavior in one or more of the phases in these models. Furthermore, little has been done in understanding the transient aspect of these models.

Gwyn et al. (1970) considered the transient behavior of the upward and downward flow of gas reactants and solid catalyst in the emulsion phase of the fluidized bed. They assumed that the flow pattern in all phases is plug flow type, the chemical reaction is linear, and physical properties are constant along the bed. Fan and Fan

---

Detailed information regarding numerical values for simulation can be obtained from the authors.

0001-1541-80-2603-0138-$00.75. © The American Institute of Chemical Engineers, 1980.